





Elucidation of the de Vries behavior in terms of the orientational order parameter, apparent tilt angle, and field-induced tilt angle for smectic liquid crystals by polarized infrared spectroscopy

Neelam Yadav,^{1,2} V. Swaminathan ,¹ V. P. Panov ,^{1,3} R. Dhar ,² and J. K. Vij ^{1,*}

¹Department of Electronic and Electrical Engineering, Trinity College Dublin, University of Dublin, Dublin 2, Ireland

²Centre of Materials Sciences, University of Allahabad, Allahabad, India

³Department of Electronic and Computer Engineering, Sungkyunkwan University, Jangan-Gu, Suwon, Republic of Korea



(Received 20 August 2019; published 27 November 2019)

We report experimental results of the orientational order parameter, the apparent tilt angle, and the field-induced tilt angle for three chiral smectic liquid crystalline materials investigated using infrared (IR) polarized spectroscopy. The common feature in these materials is use of the core 5-methyl-2-pyrimidine benzoate as the central part of the mesogen. This core is terminated by siloxane or carbosilane chains on one of the ends and by the chiral alkoxy chains on the opposite. These compounds exhibit low concomitant layer shrinkage at the smectic A^* (SmA^*) to smectic C^* (SmC^*) transition temperature and within the SmC^* phase itself. The maximum layer shrinkage in SmC^* is observed as $\sim 1.5\%$. We calculate the apparent orientational order parameter, S_{app} in the laboratory reference frame from the observed IR absorbance for homeotropic aligned samples, and the true order parameter, S , is calculated using the measured tilt angle and is also interpolated from Iso- SmA^* transition temperature closer to SmC^* phase. The apparent tilt angle in the SmA^* phase calculated from a comparison of order parameters S and S_{app} is found to be significantly large. A low magnitude of S_{app} found for homeotropic aligned samples in the SmA^* phase indicates that the order parameter plays a vital role in determining the de Vries characteristics, especially of exhibiting larger apparent tilt angles. Furthermore there is a significant increase in the true order parameter at temperatures close to SmA^* to SmC^* transition temperature in all three compounds. The planar-aligned samples are used to study the dependence of induced tilt angle on the applied electric field. The generalized Langevin–Debye model given by Shen *et al.* reasonably fits the experimental data on the field-induced tilt angle. The results show that the dipole moment of the tilt correlated domain in SmA^* diverges as temperature is lowered to the $SmA^* - SmC^*$ transition temperature. The generalized Langevin–Debye model is also found to be extremely effective in confirming some of the conclusions of the de Vries behavior.

DOI: [10.1103/PhysRevE.100.052704](https://doi.org/10.1103/PhysRevE.100.052704)

I. INTRODUCTION

Liquid crystals constituted of calamitic rodlike mesogens and long chains attached to the two ends of the mesogen normally form smectic phases. Smectic liquid crystalline phases are perceived as one-dimensional piling up of the two-dimensional fluid layers, where the single dimension is denoted by the density wave vector [1,2]. The layer normal is parallel to the density wave vector; the positional and the orientational order parameters govern the characteristics of smectic liquid crystals. The long molecular axis is almost collinear with the director in smectic A (SmA) phase similar to that in a nematic phase, whereas in the smectic C (SmC) phase, the director is tilted with respect to the layer normal. If the molecules are optically active, SmC phase is chiral and the spontaneous polarization emerges normal to the tilt plane, where the latter is constituted by the director and the layer normal [3]. The director forms a helicoidal structure in which the helical axis lies parallel to the layer normal [4]. The pitch of the helix so formed lies generally in the optical wavelength range.

Based on an extensive study of the SmA to SmC transition of most smectics [5–11] it has been inferred that a continuous transition from SmA to SmC phase can be described by a complex number $\psi (= \Theta e^{i\phi})$, where Θ is the magnitude of the tilt angle of the director from the layer normal and ϕ is the azimuthal angle of the direction of the tilt. However, it should be emphasized that the disorder-order type transition had been considered as a useful basis, especially in relation to the molecular biaxiality [12,13], and in explaining a small change in the layer thickness at the SmA^* to SmC^* transition temperature. Such a transition may thus be important for exploring the first-order or weakly first-order transitions. De Jeu *et al.* [14] and Adriaan de Vries [15] reported that the SmA to SmC transition in some smectics such as 70.5 could be of the disorder-order type because x-ray diffraction studies revealed a negligible change in the smectic layer spacing at the transition temperature. They found that the long molecular axis is tilted by an angle of $\sim 16^\circ$ from the layer normal, at a temperature close to the transition temperature. Furthermore the orientational order parameter in SmA is significantly lower than unity. An importance of the orientational order parameter (S) on the layer spacing first realized by Leadbetter and Richardson provided the basis of de Vries' work. Different models, as slight variants of one another, are noncorrelation, symmetric, asymmetric, and diffuse cone.

*Corresponding author: jjvij@tcd.ie

These were proposed to explain the various experimental results obtained by de Vries [16–18]. Out of these models, the diffuse cone, is the most widely accepted one. In this model, de Vries considered a probability distribution function, $P(\Theta) = b \sin \Theta \exp[f(T)\cos^2\Theta]$. The suggestion of an importance of the orientational order parameter based on the Maier-Saupe model for nematics made initially by Leadbetter and Richardson inspired de Vries to insert $\cos^2\Theta$ term in the above distribution function [19]. According to this model, the director is tilted with respect to the layer normal in the SmA phase, but it is distributed randomly to form a diffuse cone in order to ensure the uniaxiality of SmA phase. The characteristics of de Vries smectics are thus quite distinct from those of a conventional smectic A phase. At the SmA to SmC transition, the rotational symmetry of the azimuthal distribution is lost, and consequently the net molecular tilt angle increases sharply with a reduction in temperature. The compounds that use siloxane or carbosilane end chains exhibit nanophase separation, and the large field-induced tilt angles observed in SmA* usually reflect de Vries characteristics [20–24].

The main objective of this paper is to find roles of the orientational order parameter and of azimuthal distribution of the director, in determining the de Vries smectic characteristics of large (1) apparent as well as (2) field-induced tilt angle in the SmA* phase found in three compounds, DR276, DR118, and DR133, and to determine their role in the smectic layer spacing. We use the characterization technique of polarized infrared spectroscopy. We calculate the apparent order parameters S_{app} for homeotropically aligned samples in the laboratory frame and then proceed to measure the real order parameter (S) by using the experimentally obtained values of tilt angle near to the SmA* to SmC* transition using the interpolated procedure described here. Finally we determine the apparent tilt angle for the entire range of temperatures in the SmA* phase and SmC* phases. Results of the field-induced tilt angle on the applied voltage (electric field = voltage/cell spacing) are presented for homogeneously aligned liquid crystalline samples. The obtained induced-tilt angle is fitted to the theoretical model in order to elucidate the de Vries scenario.

II. EXPERIMENT

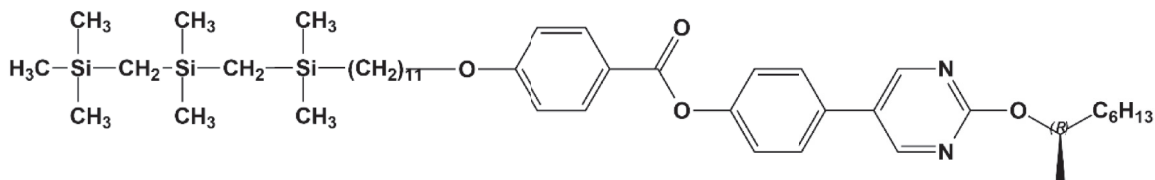
A. Materials

The chemical formulae, phase sequences, and phase transition temperatures of three compounds, DR276, DR118, and DR133, are given in Fig. 1. The compounds DR276 and DR133 use 5-phenyl 2-pyrimidine benzoic acid core. The core for both compounds is terminated by tricarbosilane undecyloxy and trisiloxane-undecyloxy chains for DR276 and DR133, respectively, on one of their ends. On the opposite end, the core for all the three compounds is terminated by a chiral alkyloxy tail, and the CH₃ group is attached to the chiral carbon atom. Carbosilane or trisiloxane groups together with the (CH₂)₁₁ spacer promote nanophase separation and facilitate formation of the smectic C phase. In DR118, however, the ester group that links the two phenyl rings in the mesogen is absent. Similarities in the molecular structures of these compounds thus include terminations by the chiral alkoxy chain on one of the ends and the bulky siloxane or

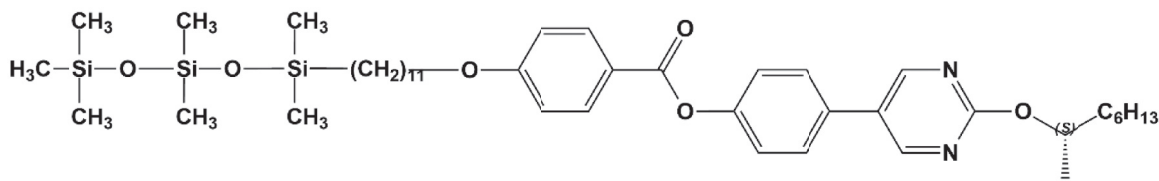
carbosilane tail on its opposite ends. The latter as suggested earlier gives rise to a nanophase sublayer-like separation and lamellar ordering with a well-defined layer structure. Bulky carbosilane and siloxane groups are also known to promote SmC phase [25]. An esterified molecular core in DR133 enhances the mesogen's polarity and creates flexibility in the molecular conformation [26], whereas the methyl group to the chiral carbon atom leads to the emergence of the spontaneous polarization [27] in the three cases. It has been found that silicon or fluorine termination also promotes de Vries-like smectic behavior [28,29].

B. Infrared spectroscopic measurements

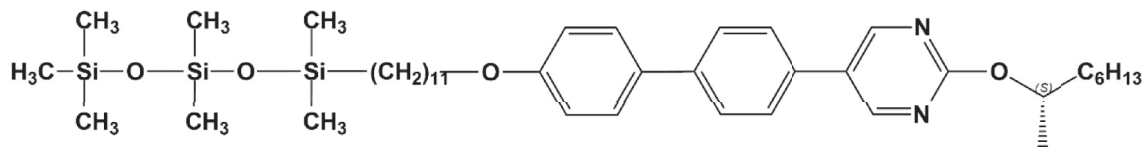
The polarized infrared (IR) spectroscopic measurements are carried out using a Bio-Rad FTS-6000 spectrometer. The investigated spectral range extends from 450 to 4000 cm⁻¹. The spectrometer is equipped with a liquid-nitrogen-cooled mercury cadmium telluride detector of IR radiation and a computer-controlled wire grid rotation polarizer. A hot stage with a temperature stability of better than ± 0.02 °C forms a part of the experimental measuring setup. An average of 64 scans of the spectra is recorded. This gives rise to a spectral resolution of 2 cm⁻¹ and to the signal-to-noise ratio higher than 2000. The cell preparation techniques include the adoption of careful procedures for obtaining both homeotropic and planar alignments of compounds on the windows of the cell. For both alignments, zinc selenide windows with a thin layer of indium tin oxide sputtered on to them are used in an IR liquid crystalline cell. A Mylar spacer of 5 μ m thickness separates the two overlapping windows. For achieving a “planar alignment,” both windows are coated with polymer solution RN1175 (Nissan Chemicals), following which the windows are kept in a vacuum oven at 250 °C for 1 h. The aligning solution on the windows is thus polymerized by baking, and this forms a thin planar-alignment layer. The alignment layers of the cell are rubbed antiparallel using a commercial rubbing machine. For obtaining the homeotropic alignment layer, the windows are coated with the solution of chromolane in ethyl alcohol. The alignment layer is subsequently cured for 1 h at a temperature of 120 °C, which also allows the alcohol to evaporate. The IR spectra are recorded for different temperatures and especially for smaller increments in temperature of 0.5 °C close to the SmA* to SmC* phase transition temperature. DC bias voltages of both polarities are applied across the electrodes of the IR cell. The polarizer is rotated from an angle of 0° to 180° in steps of 20°. For each step of the polarizer direction, the IR spectra are recorded as a function of the applied voltage. This procedure is repeated for different temperatures of the sample in the cell. A Voigt function is used to fit the absorbance profile of the phenyl ring C-C stretching mode at 1605 cm⁻¹ for each applied voltage and temperature. The Perkin Elmer Grams Research program is used to find the intensity and the spectral width of the recorded spectral line, and the Origin-8 program is used to fit each absorbance profile to the Voigt function. The thickness of the fabricated cells prior to their fillings is measured using a UV-VIS spectrometer (Avaspec-2048) based on using the technique of the interference of waves that produce fringes and commercial software.



Cr 14°C Sm X 48°C Sm C^* 78.5°C Sm A^* 87°C I (**DR276**)



Cr 11°C Sm C^* 94°C Sm A^* 102°C I (**DR133**)



Cr 60°C Sm C^* 95°C Sm A^* 113°C I (**DR118**)

FIG. 1. Molecular structures of the compounds DR276, DR133, and DR118 and the transition temperatures determined by differential scanning calorimetry (DSC) are given. The phase transition temperatures are also obtained by polarized optical microscopy. The cooling rate used for both techniques is 1 °C/min.

III. RESULTS AND DISCUSSIONS

Three homeotropically aligned cells are prepared by filling each cell with a different compound to be investigated. Infrared spectroscopic measurements are made on aligned sample cells after each cell in turn is carefully mounted in the hot stage fixed to the rotation table of the optical polarizing microscope.

A. Results on homeotropically aligned IR cells

Before carrying out IR measurements, sample textures are recorded with a polarizing optical microscope. Single-domain textures are observed in the Sm A^* phase. The texture confirms perfect homeotropic alignment in each case. Multidomain textures attributed to the azimuthal freedom of the tilting directions are observed at the Sm A^* – Sm C^* transition temperature. Infrared measurements exhibit an absence of IR dichroism in the Sm A phase. This indicates that the azimuthal angle made by the director on the substrate surface can take all values ranging from 0 to 2π with equal probability. Absorbance profile is normally independent of the projection of the director onto the plane of the windows

when the spectral profile is integrated over an area of the IR beam of diameter $<10\ \mu\text{m}$. Figures 2(a)–2(c) illustrate the normalized absorbance of the C-C stretching phenyl vibration band ($\frac{A_{\text{per}}}{A_{\text{iso}}}$), the absorbance due to a projection of the square of transition moments along the windows of the cell normalized by the similar absorbance measured in the isotropic phase. The phenyl band is chosen due to its transition dipole moment being almost collinear with the long molecular axis. As the sample cell is cooled from isotropic phase to Sm A^* phase, a sudden drop in the absorbance is detected with temperature. This demonstrates a sudden decrease in the projections of the square of the transition dipole moments normal to the direction of IR beam, brought about by an almost perfect homeotropic alignment of the mesogens onto the substrates. In the vicinity of the phase transition temperature I-Sm A^* , the absorbance is observed to decrease sharply with a decrease in temperature close to the I-Sm A^* transition in DR133, and in other two cases the decrease occurs over a range of 2–3 °C in temperature and after the Sm A^* – Sm C^* transition temperature the absorbance rises gradually. This observation implies a progressive increase in the apparent tilt angle of the mesogens in the Sm A^* phase, and it increases further

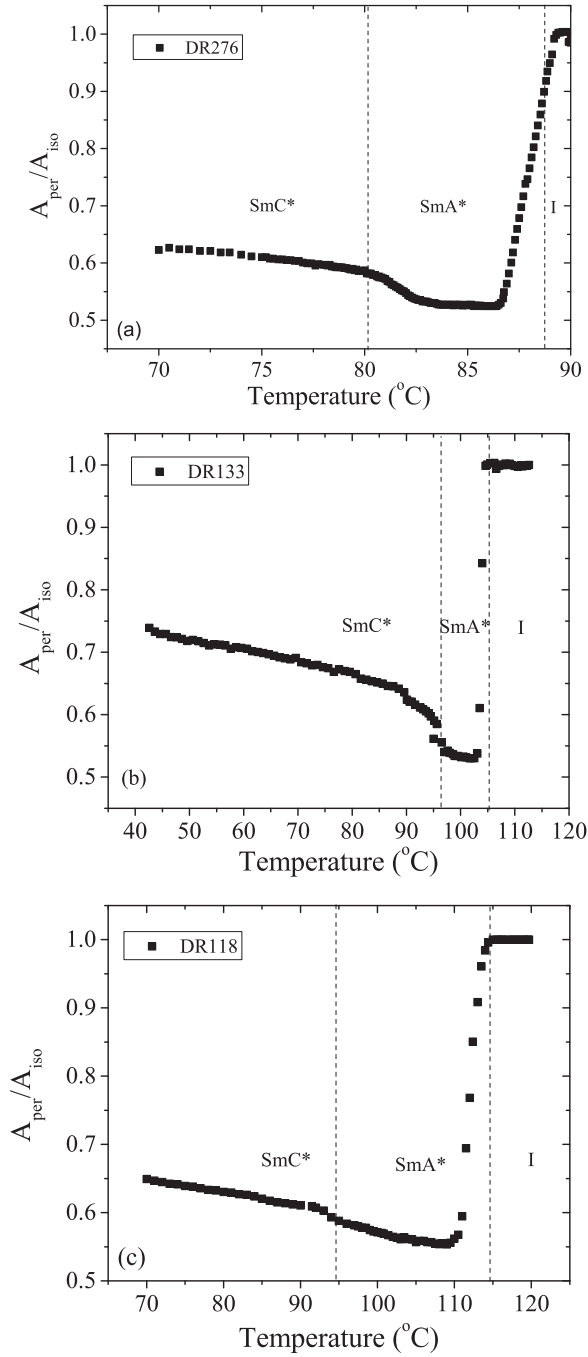


FIG. 2. Absorbance of the phenyl band as a function of temperature/phase for (a) DR276, (b) DR133, and (c) DR118.

as the temperature is reduced to SmA* to SmC* transition temperature. A continuous small step increase in absorbance at the SmA* to SmC* transition is observed in these cases as opposed to a sharp increase at the transition temperature in a conventional smectic compound, C7 [30]. In SmC* phase, the absorbance displays increasing trend as temperature is lowered since the mesogens increasingly tilt with a reduction in temperature from the layer normal. The apparent orientational order parameters S_{app} in SmA* and SmC* are calculated from the experiments conducted on the homeotropically aligned samples, and these are plotted in Figs. 3(a)–3(c) for the compounds DR276, DR133, and DR118.

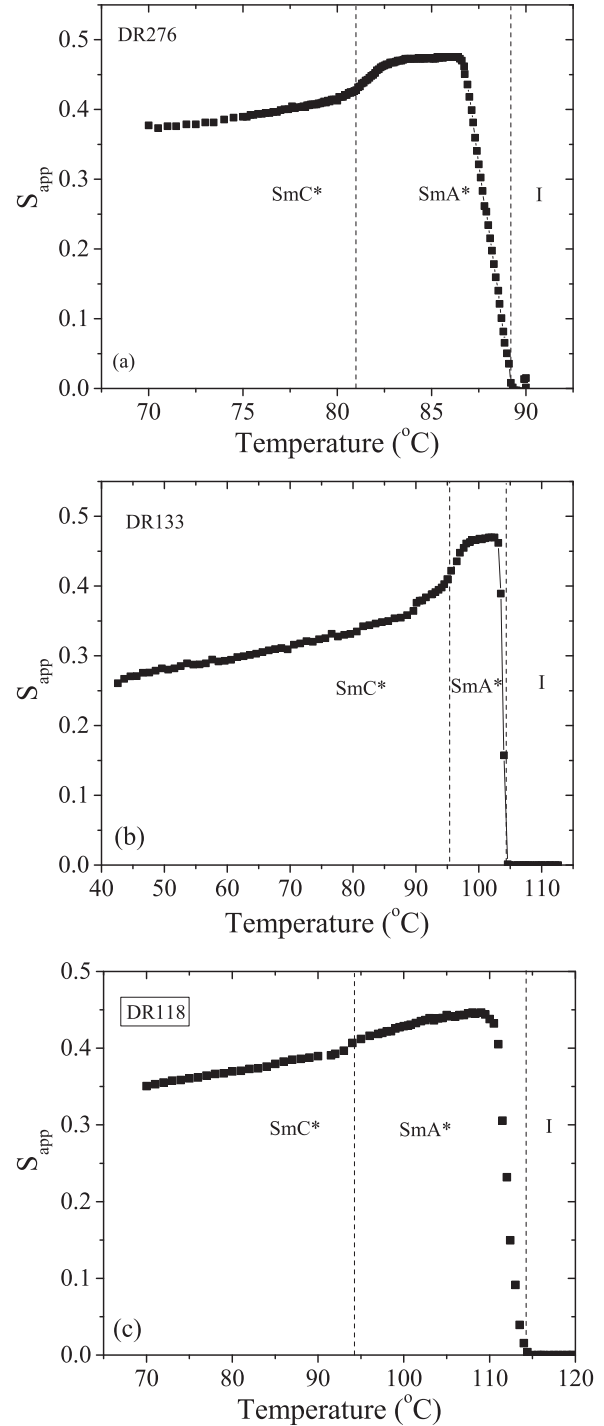


FIG. 3. Variation of the apparent order parameter (S_{app}) with temperature for homeotropically aligned cells of (a) DR276 (b) DR133, and (c) DR118.

In the experiment on a homeotropic aligned LC cell, the IR beam is incident parallel to the smectic layer normal. In the laboratory frame of reference, IR absorbance is given by [31,32]

$$A_{\text{per}}/A_{\text{iso}} = 1 - S_{\text{app}}P_2(\cos \beta_l) + \frac{1}{2}D_{\text{app}}\sin^2 \beta_l \cos 2\gamma_l, \quad (1)$$

where the apparent orientational order parameter, for the long and the short molecular axes, is S_{app} and D_{app} (the latter is

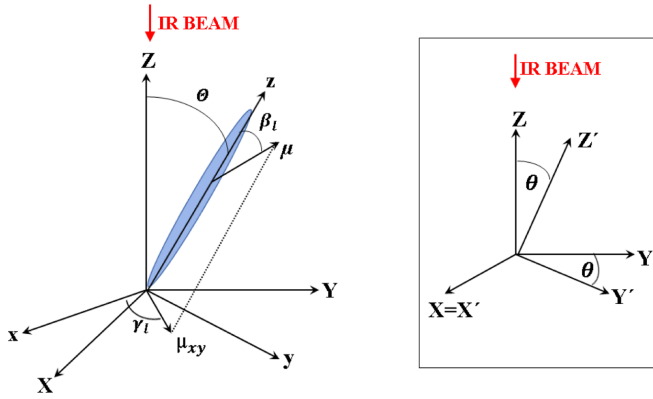


FIG. 4. Representation of experiments performed on homeotropically aligned samples. X , Y , and Z denote the axes of the laboratory frame of reference; x , y , and z are the axes of the molecular reference frame. Θ is one of the Euler angles which describe the orientation of the molecular reference frame versus the laboratory reference frame. The direction of the IR transition dipole moment μ relative to the long axis of mesogens in the molecular frame of reference is denoted by the polar angle β_l and azimuthal angle γ_l . The inset shows the definition of the local system described in the text: X' , Y' , and Z' are axes of the local frame of reference; θ is the in-layer tilt angle made by the director, $\theta = \langle \Theta \rangle$ (averaging is done for a single smectic layer).

also the molecular biaxiality order parameter), respectively. $P_2(\cos \beta_l) = \frac{1}{2}(3\cos^2 \beta_l - 1)$ is the second Legendre polynomial. The direction of the IR transition dipole moment relative to the long axis of mesogens in the molecular frame of reference is denoted by the polar angle β_l and azimuthal angle, γ_l . Since $\beta_l < 6^\circ$ for the phenyl C-C stretching vibration band, two $\sin^2 \beta_l$ terms in Eq. (1) contribute only 1% of the total absorbance, and hence these terms can be neglected. We thus approximate Eq. (1) as

$$S_{\text{app}} \approx 1 - \frac{A_{\text{per}}}{A_{\text{Iso}}}. \quad (2)$$

The apparent orientational order parameter in the laboratory frame of reference, S_{app} , is thus calculated using Eq. (2) from the normalized absorbance.

Locally, the symmetry of the distribution function changes from uniaxial to biaxial at the SmA^* to SmC^* transition temperature at the level of a single smectic layer. In this case, the tilt plane formed by the director and the smectic layer normal is the only plane of symmetry of the system. For the tilted smectic phases, however, the most convenient option is to choose a reference frame fixed to the local director and to the tilt plane. A new reference frame called the local frame is thus obtained from rotating the laboratory frame of reference by an angle θ about the X axis (see Fig. 4). In this local frame of reference, $P = 0$, and S is the true molecular order parameter as for the nematics. The tilt affects the magnitude of the order parameters. Finally, the absorbance in the local frame of reference is written as [32,33]

$$A = \frac{1}{2}[A_Z \sin^2 \theta + A_Y \cos^2 \theta + A_X]. \quad (3)$$

where A_X , A_Y , and A_Z are components of absorbance that are now described by S , D , and P in the new frame of reference.

Further, the above equation is [32]

$$A = 1 - SP_2(\cos \theta)P_2(\cos \beta_l) + \frac{1}{2}[DP_2(\cos \theta) - \frac{1}{2}C \sin^2 \theta] \sin^2 \beta_l \cos 2\gamma_l, \quad (4)$$

where C is the mixed biaxiality used to denote coupling between D and P . S , D , and C denote the true order parameters in the new chosen reference system.

On comparing Eqs. (1) and (4), we find that the apparent orientational order parameter is equal to the true orientational order parameter (S) of the molecules, multiplied by $P_2(\cos \theta)$ [32]:

$$S_{\text{app}} = S P_2(\cos \theta), \quad (5)$$

where $P_2(\cos \theta)$ is the second-order Legendre polynomial of the tilt angle θ . S_{app} is measured in the laboratory frame. We use values of the experimentally calculated tilt angles near the $\text{SmA}^* - \text{SmC}^*$ transition temperature, and the measured values of S_{app} , S (solid green triangles in Fig. 5) are calculated from the tilt angle. Results for S for the three compounds at temperatures close to the $\text{SmA}^* - \text{SmC}^*$ transition temperature are plotted in Fig. 5. The interpolated values of S (red circles) for the remaining temperatures by assuming zero tilt angle at the I to SmA^* phase transition temperature are obtained by using the following equation [33]:

$$S = S_{\text{app}} + A\tau^\beta, \quad (6)$$

where β , A are constants.

Here $\tau = 1 - T/T_{I-\text{SmA}^*}$, where τ is the reduced temperature, and $T_{I-\text{SmA}^*}$ is the isotropic (I) to SmA^* transition temperature. Experimentally, it is found that the apparent order parameter for the short axis or the molecular biaxiality order parameter (D_{app}) is negligible at the I to SmA^* transition, and an assumption of the zero tilt angle at I- SmA^* transition temperature is therefore justified. The calculated value acts as the lower bound values of the tilt angle by noting that this angle cannot be less than zero. Finally, the tilt angle for the entire range of temperatures is calculated using Eq. (5) and using interpolated Eq. (6) for specified points and the actual values of S as discussed above. From these results, we infer that the mesogen is tilted by a finite angle in the SmA^* phase of DR276, DR133, and DR118. As the angle is large enough, de Vries behavior is confirmed.

B. Planar-aligned samples

Here we present results of the measurements on the absorbance profile for a planar-aligned cells as a function of the electric field across the cell. Figure 6 gives the optical textures for DR118 at different voltages, as an example, the quality of the alignment is found to be high. The IR spectra are recorded for each temperature by varying the magnitude of the negative and positive voltages. The corresponding absorbance profiles $A(\Omega_p)$ for the C-C phenyl stretching vibrations as a function of the angle by which the polarizer is rotated under the application of the positive and negative DC voltages are determined. Figure 7 shows a polar plot of A with respect to Ω_p plotted by using the experimental data for the opposite polarities of the applied DC voltage, as an example. A unique absorbance profile is created for each temperature and applied

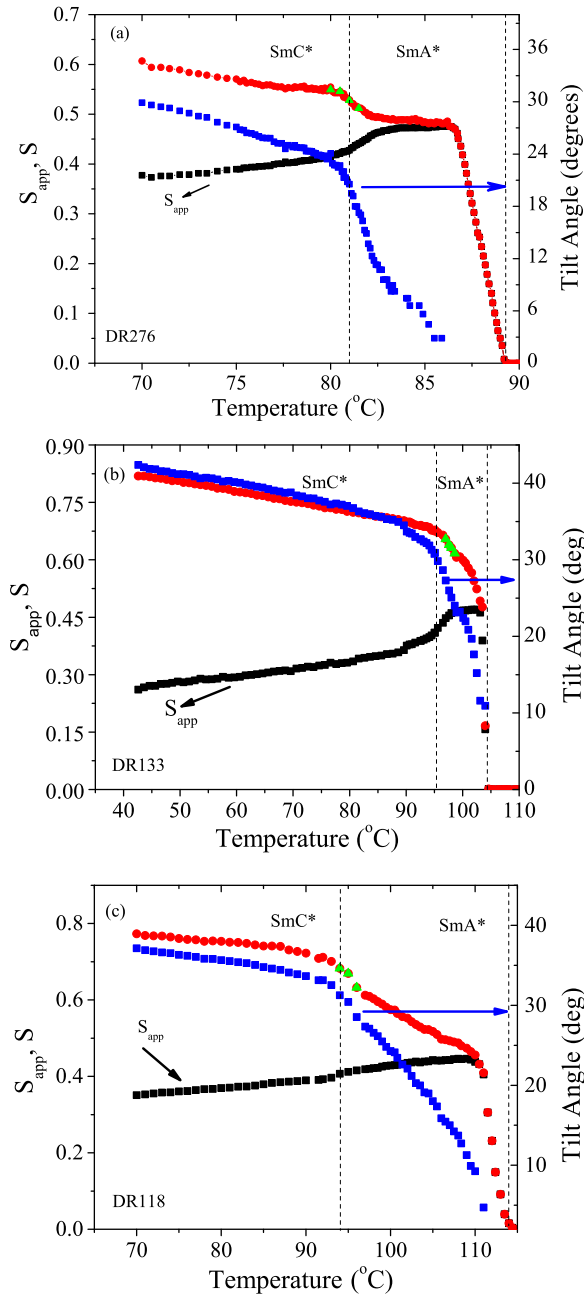


FIG. 5. Results of the order parameters for (a) DR 276 (b) DR133, and (c) DR118: The apparent order parameter (S_{app}) [black squares] calculated with respect to the fixed laboratory frame of reference, the green triangles denote the true order parameter, S , calculated by using Eq. (5) and the experimentally obtained tilt angles measured close to the SmA^* to SmC^* transition temperature, and red filled circles denote the interpolated values of S . These order parameters are used to calculate the apparent molecular tilt angle (blue squares) plotted for the entire range of temperatures in a homeotropically aligned cell.

voltage and is fitted to the following equation [24,34]:

$$A(\Omega_p) = -\log_{10}[10^{-A_{\parallel}} + (10^{-A_{\perp}} - 10^{-A_{\parallel}})\sin^2(\Omega_p - \Omega_{max})]. \tag{7}$$

The angle the polarizer makes with a reference direction is denoted by Ω_p . The highest values of the absorbance of a band

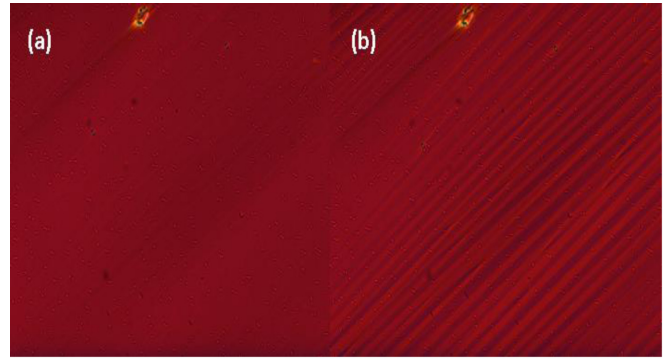


FIG. 6. Optical textures of planar-aligned sample of DR276 for two temperatures (a) 84 °C, 0 V and (b) 85 °C at 40 V in the SmA^* phase.

are given by A_{\parallel} for $\Omega_p = \Omega_{max}$. For the polarizer angle, $\Omega_p = 90^\circ + \Omega_{max}$ the absorbance for the phenyl C-C stretching band is a minimum and is denoted by A_{\perp} . Equation (7) is fitted to the polar plots obtained for different temperatures and different voltages of opposite polarities. The fit gives values of Ω_{max} for which the absorbance is a maximum for a fixed voltage. The induced IR tilt angle (Ω_{ind}) as a function of Ω_{max} for positive and negative applied voltages. The de Vries smectics with a chiral carbon are known to display unusual electro-optical characteristics, in terms of the apparent tilt angle and the birefringence. These are modeled using several approaches [35–37]. Clark *et al.* used the Langevin-Debye model to qualitatively elucidate the electro-optical properties of the smectics. Initially, the same Langevin-Debye model was proposed by Fukuda *et al.* [38] to explain the V-shaped switching in an antiferroelectric liquid crystal. The Clark model is based on the assumption that the mesogens are distributed over a cone of a fixed cone angle in the absence of an applied electric field [39] in the SmA^* phase. On application of an electric field (E_{ap}), the free energy includes the term involving the proportionality factor of the local dipole moment (p) and the azimuthal angle, $pE_{ap}\cos\phi$. However, this approach

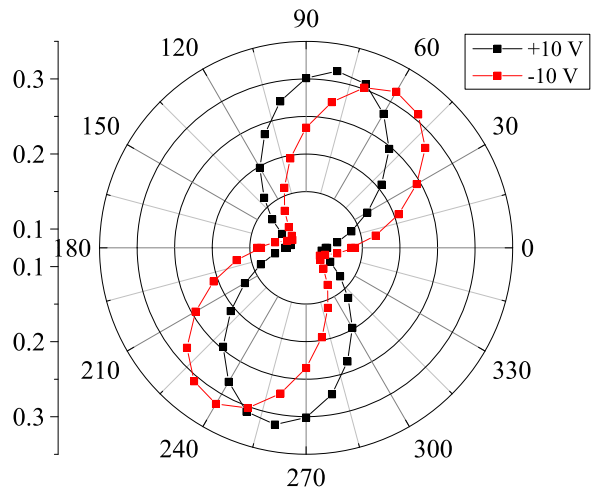


FIG. 7. Polar plots of the absorbance profile in terms of the polarizer angle for the compound DR118, as an example.

though successful in general did prove short of explaining the experimentally observed sigmoidal response of tilt angle as function of the electric field obtained. Following this, Shen *et al.* introduced a quadratic term in the field in the free energy function for the orientational distribution of the mesogens having a term dependent on E_{ap} of the second order with two degrees of freedom: azimuthal φ as well as the tilt (Ω) angles. This model was called the generalized Langevin-Debye model [40]. Shen *et al.* constrained the values of $\Omega(E_{ap})$ to change within specified narrow range of values. The experimental results determined the upper and the lower limiting values of Ω . The birefringence value in the absence of electric field sets the lower limit for Ω_{\min} while the maximum angle Ω_{\max} for large applied fields determines the upper limit. The expression of the free energy function in the generalized Langevin-Debye model is written in the form [40]

$$\begin{aligned}
 U &= -\mathbf{p} \left(1 + \alpha \frac{\mathbf{p}}{|\mathbf{p}|} \cdot E_{ap} \right) \cdot E_{ap} \\
 &= -p_0 E_{ap} \sin \Omega \cos \varphi (1 + \alpha E_{ap} \cos \varphi), \quad (8)
 \end{aligned}$$

where $\mathbf{p} = p_0 \sin \Omega$ denotes the mean value of the dipole moment of the domain having the azimuthal angle, which is not degenerate. The first term on the right-hand side of Eq. (8) accounts for the free energy related to the interactions of the dipoles with E_{ap} . The second term quadratic in E_{ap} is associated with the scaling phenomenological parameter (α). The tilt susceptibility for the sigmoidal response seen in the plot of the experimental data of the tilt angle as a function of E_{ap} is described by the quadratic term. The mean field molecular orientational distribution function can be defined as

$$\begin{aligned}
 f(\Omega, \varphi) &= \exp[-U/k_B T] / \int_{\Omega_{\min}}^{\Omega_{\max}} \int_0^{2\pi} \exp[-U/k_B T] \\
 &\quad \times \sin \Omega d\Omega d\varphi. \quad (9)
 \end{aligned}$$

The average value of a physical parameter $\langle X \rangle$ can be calculated from the given molecular distribution using the following equation:

$$\langle X \rangle = \int_{\Omega_{\min}}^{\Omega_{\max}} \int_0^{2\pi} X(\Omega, \varphi) f(\Omega, \varphi) \sin \Omega d\Omega d\varphi. \quad (10)$$

Further, the dielectric tensor is averaged and is diagonalized in the laboratory frame of reference to derive the electric field dependent optical tilt $\Omega_{\text{ind}}(E_{ap})$ as

$$\tan 2\Omega_{\text{ind}} = \frac{\langle \sin 2\Omega \cos \varphi \rangle}{\langle \cos^2 \Omega - \sin^2 \Omega \cos^2 \varphi \rangle}. \quad (11)$$

The dependence of the apparent tilt angle for IR (Ω_{ind}) found from a set of Eqs. (8) to (11) on electric field at temperatures close to the SmA^* to SmC^* transition for DR276, DR118, and DR133 are plotted in Fig. 8. It is similar to the plots of the apparent optical tilt found as (Θ_{ind}) and birefringence Δn [21,41,42] by using the automated time-resolved polarimeter technique as a function of the electric field. The parameters of fit are found. The layer shrinkage, molecular tilt, and birefringence of these three compounds are

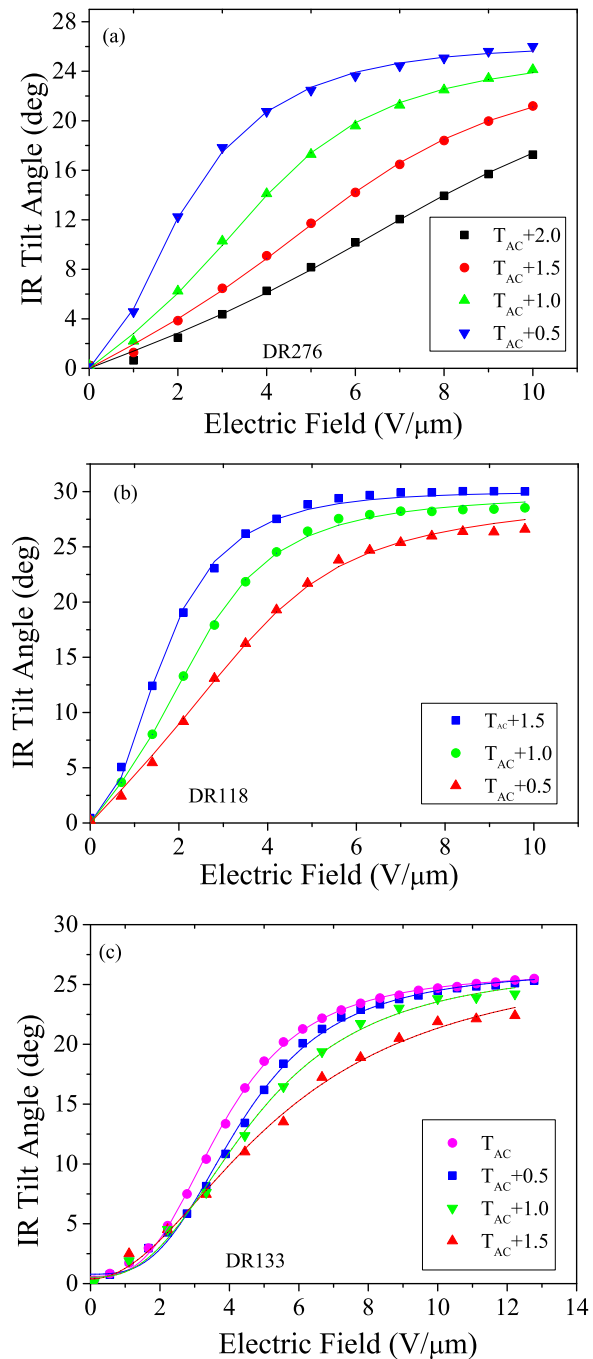


FIG. 8. The voltage dependence of the molecular IR tilt angle (Ω_{ind}), determined from the absorbance profiles of the C-C phenyl ring stretching vibration at different temperatures in the SmA^* phase close to the $\text{SmA}^* - \text{SmC}^*$ transition for (a) DR276 (b) DR118, and (c) DR133 at 1605 cm^{-1} , respectively. The symbols correspond to the experimental data, and the solid lines are fits to the generalized Langevin-Debye model given in Sec. III B. The thickness of the sample is $5 \mu\text{m}$.

summarized in Table I. A plausible connection between the apparent tilt angle and birefringence had first been suggested by Lagerwall *et al.* [43]. The plots show that Ω_{ind} is low for higher temperatures in the SmA^* phase and the plot displays a linear trend on the applied electric field. However, as the

TABLE I: de Vries characteristics of DR276, DR1118, and DR133.

Material	Layer shrinkage ^a	Reduction factor ^a	Layer spacing (\AA) ^a	Optical tilt (Θ_{ind}) ^a	IR tilt angle	p_o (Debye)
DR276	1.9%	0.3	44	26.6°	25°	790
DR133	1.7%	0.3	41.6	34.5°	26°	650
DR118	1.2%	0.2	42.4	35.5°	30°	1570

^aThese values are obtained from Refs. [21] and [42].

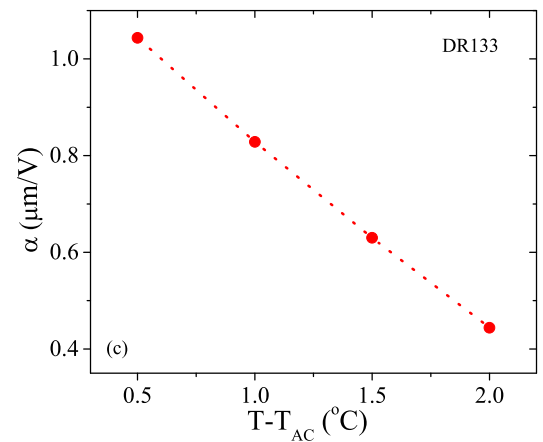
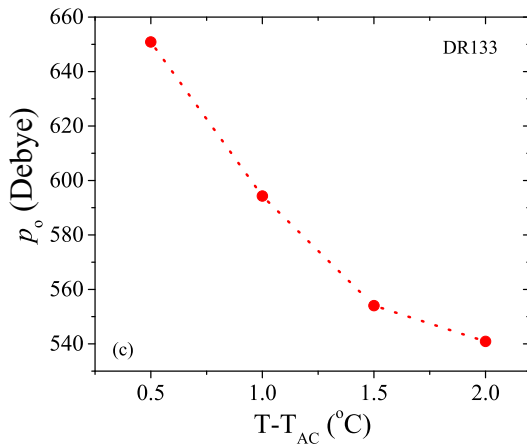
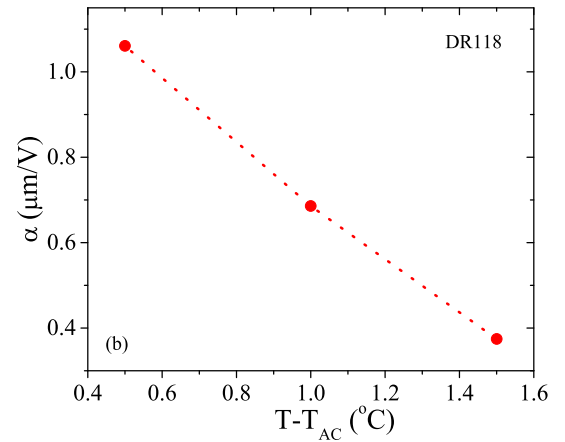
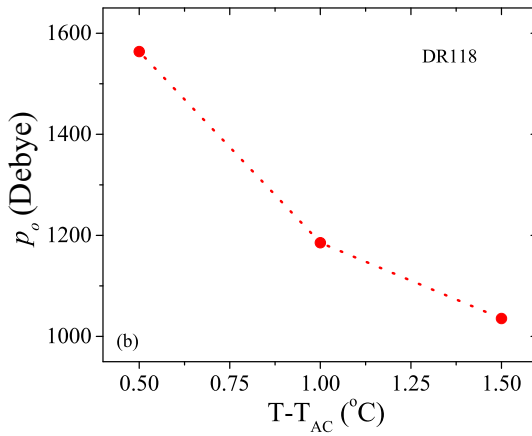
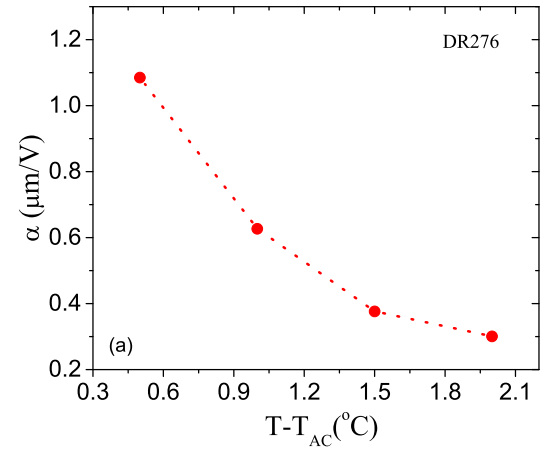
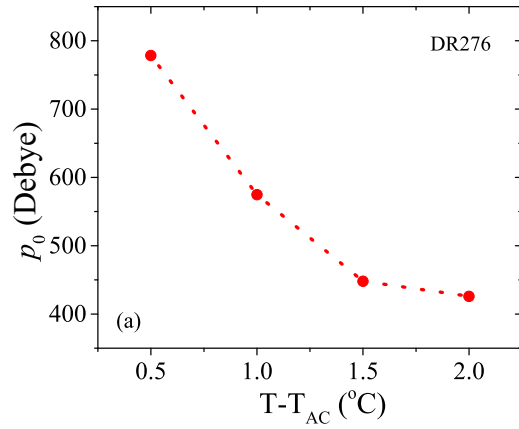


FIG. 9. The local dipole moment p_o obtained from the fitting of the experimental data to the Shen *et al.* model plotted as a function of the temperature in the SmA* phase for (a) DR276, (b) DR118, and (c) DR133.

FIG. 10. Plots of the temperature dependence of the phenomenological scaling factor α for (a) DR276, (b) DR118, and (c) DR133.

temperature reaches the SmA* to SmC* transition temperature, there is dramatic enhancement in the electro-clinic response even at low applied electric fields, and the plot turns out to be nonlinear. This is a signature of a large cone angle and a large pretransitional effects. In the vicinity of the transition temperature T_{AC} , Ω_{ind} increases rapidly to a value of $\sim 23^\circ$ and then continues to rise gradually with the applied field, finally attaining a saturation at a value of 27° in the SmA* phase. Therefore, the response is sigmoidal in shape rather than of the Langevin type; the latter is commonly observed in conventional smectics.

The experimental values of the tilt angle obtained by IR spectroscopy, i.e., Ω_{ind} , have been fitted to the generalized Langevin-Debye model using Eq. (11). The plots indicate that the optical tilt saturates at 30° : $\Omega_{max} = 30^\circ$ for DR118 and at 25° and 26° for DR276 and DR133, respectively. The dependence of the fitting parameters p_0 , and α on temperature for the three compounds approaches a maximum value close to the SmA* to SmC* phase transition. This increase can be attributed to an increase in the size of the tilt-correlated domain. DR118 has the highest value of p_0 : 1050 Debye at 95.5°C and increases to 1570 Debye at 94.5°C , while DR133 has the lowest value of 540 Debye at 94.5°C and 650 Debye at 93°C as shown in Figs. 9(a)–9(c). Figure 10 represents the plots of scaling parameter α with respect to temperature. The phenomenological scaling parameter α exhibits a linear increase as temperature is decreased from I to the SmA* to SmC* phase transition temperature. Its value lies within a range of 0.4 to 1.2 for all the three compounds.

Our results support the finding that the orientational distribution function is of the diffuse cone type rather than of the sugar loaf as found [44] experimentally from the x-ray small and large angle scattering measurements. It is suggested that the x-ray scattering presumably arises from the entire molecule rather than from the central core part of the mesogen as in IR measurements. In addition, it is found from the results and the ensuing discussion that the orientational order parameter plays a key role in leading to the de Vries characteristics. The properties of de Vries smectics are found to be different from conventional smectic liquid crystals.

IV. CONCLUSIONS

The technique of polarized IR spectroscopy gives results for the orientational order parameters, the interpretation of which advances the understanding of the de Vries smectics. The three mesogens described here exhibit de Vries-like characteristics of having (1) a significantly large electro-clinic response, (2) a low orientational order parameter in SmA*, and (3) large apparent tilt angles in the SmA* phase. The orientational order parameter for these compounds is found to be low in magnitude (less than 0.5) in the SmA* phase in comparison to the conventional smectics (~ 0.8). This implies that a large apparent tilt angle emerges in the SmA* phase. The true order parameter increases significantly close to the SmA* – SmC* transition temperature, whereas it jumps at the transition temperature and finally saturates at low temperatures. These findings confirm the validity of the theory of Saunders *et al.* [45] on de Vries materials proposed a decade ago. The dependence of the field-induced tilt angle on the applied electric field is explained by the generalized Langevin-Debye model of Shen *et al.* The results provide a clear evidence of the applicability of the diffuse-cone model of de Vries elucidated by Shen *et al.* [40] in which the cone tilt angle is restricted to lie within a range of values in between Ω_{min} and Ω_{max} . These are the two limiting values of the apparent tilt angle with temperature or field. The dependence of the apparent tilt angle on the applied electric field strikingly resembles the large dependence of the observed tilt angle on the field measured in electro-optical experiments [46].

ACKNOWLEDGMENTS

This work was partially supported by 13/US/I2866 from Science Foundation Ireland as part of the US–Ireland Research and Development Partnership program jointly administered with the U.S. National Science Foundation under Grant No. NSF-DMR-1410649. The authors thank Prof. Satyendra Kumar most sincerely for coordinating the project. V. Panov's work was partially supported by Brain Pool Program through the National Research Foundation of Korea (NRF) funded by the Ministry of Science and ICT (Grant No. 2019H1D3A2A02060963).

-
- [1] S. T. Lagerwall, Ferroelectric liquid crystals, in *Handbook of Liquid Crystals: Smectic and Columnar Liquid Crystals*, edited by J. W. Goodby, P. J. Collings, T. Kato, C. Tschierske, H. F. Gleeson, and P. Raynes (Wiley-VCH, Weinheim, 2014), Vol. 4, pp. 1–258.
- [2] J. P. F. Lagerwall and F. Giesselmann, Current topics in smectic liquid crystal research, *Chem Phys. Chem.* **7**, 20 (2006).
- [3] K. L. Sandhya, Yu. P. Panarin, V. P. Panov, J. K. Vij, and R. Dabrowski, Experimental study of de Vries properties in antiferroelectric smectic liquid crystals, *Eur. Phys. J. E.* **27**, 397 (2008).
- [4] P. G. de Gennes and J. Prost, *The Physics of Liquid Crystals* (Clarendon Press, Oxford, 1993).
- [5] S. P. Sreenilayam, D. Rodriguez-Lojo, V. P. Panov, V. Swaminathan, J. K. Vij, Yu. P. Panarin, E. Gorecka, A. Panov, and P. J. Stevenson, Design and investigation of de Vries liquid crystals based on 5-phenyl-pyrimidine and (R,R)-2,3-epoxyhexoxy backbone, *Phys. Rev. E* **96**, 042701 (2017).
- [6] M. A. Osipov and S. A. Pikin, Molecular models for the ferroelectric smectic C* phase, *Mol. Cryst. Liq. Cryst.* **103**, 57 (1983).
- [7] A. S. Govind and N. V. Madhusudana, A simple molecular theory of smectic-liquid crystals, *Europhys. Lett.* **55**, 505 (2001).
- [8] A. Poniwierski and T. J. Sluckin, Nematic, smectic-A, and smectic-C ordering in a system of parallel cylinders with quadrupolar interaction, *Molec. Phys.* **73**, 199 (1991).
- [9] W. J. A. Goossens, The smectic A and the smectic C phases: A coherent molecular picture, *Mol. Cryst. Liq. Cryst.* **150B**, 419 (1987).
- [10] M. A. Osipov, A. Fukuda, and H. Hakoi, Synclinic and anti-clinic ordering in frustrated smectics, *Mol. Cryst. Liq. Cryst.* **402**, 9 (2003).

- [11] V. Swaminathan, V. P. Panov, A. Kocot, and J. K. Vij, Molecular orientational distribution function of a chiral de Vries smectic liquid crystal from birefringence measurements, *J. Chem. Phys.* **150**, 084901 (2019).
- [12] R. J. Meyer and W. L. McMillan, Simple molecular theory of the smectic C, B and H phases, *Phys. Rev. A* **9**, 899 (1974).
- [13] W. L. McMillan, Simple molecular theory of the smectic C phase, *Phys. Rev. A* **8**, 1921 (1973).
- [14] W. H. de Jeu and J. A. de Porter, X-ray diffraction of the smectic phases of N-(p-n heptyloxybenzylidene)-p'-n-pentylaniline, *Phys. Lett. A* **61**, 114 (1977).
- [15] A. de Vries, Experimental evidence concerning two different kinds of smectic-C to smectic-A transitions, *Mol. Cryst. Liq. Cryst.* **41**, 27 (1977).
- [16] A. de Vries, A. Ekachai, and N. Spielberg, Why the molecules are tilted in all smectic A phases, and how the layer thickness can be used to measure orientational disorder, *Mol. Cryst. Liq. Cryst. Lett.* **49**, 143 (1979).
- [17] A. de Vries, The description of the smectic A and C phases and the smectic A-C phase transition of TCOOB with a diffuse cone model, *J. Chem. Phys.* **71**, 25 (1979).
- [18] A. de Vries, A. Ekachai, and N. Spielberg, X-ray studies of liquid crystals VI the structure of the structure of the smectic A, C Bn and Bt phases of trans-1,4-cyclohexane-di-n-octyloxybenzoate, *J. Phys. (Paris), Colloq.* **40**, C3-147 (1979).
- [19] A. J. Leadbetter and R. M. Richardson, Molecular motions in a smectic A phase by incoherent quasielastic neutron scattering, *Molec. Phys.* **35**, 1191 (1978).
- [20] S. P. Sreenilayam, D. M. Agra-Kooijman, V. P. Panov, V. Swaminathan, J. K. Vij, Yu. P. Panarin, A. Kocot A. Panov, D. Rodriguez-Lojo, P. J. Stevenson, M. R. Fisch, and S. Kumar, Phase behavior and characterization of heptamethyltrisiloxane-based de Vries smectic liquid crystal by electro-optics, x-rays, and dielectric spectroscopy, *Phys. Rev. E* **95**, 032701 (2017).
- [21] S. P. Sreenilayam, D. Rodriguez-Lojo, D. M. Agra-Kooijman, J. K. Vij, V. P. Panov, A. Panov, M. R. Fisch, S. Kumar, and P. J. Stevenson, de Vries liquid crystals based on a chiral 5-phenylpyrimidine benzoate core with a tri- and tetra-carbosilane backbone, *Phys. Rev. Mater.* **2**, 025603 (2018).
- [22] K. M. Mulligan, A. Bogner, Q. Song, C. P. J. Schubert, F. Giesselmann, and R. P. Lemieux, Design of liquid crystals with 'de Vries-like' properties: The effect of carbosilane nanosegregation in 5-phenyl-1,3,4-thiadiazole mesogens, *J. Mater. Chem. C* **2**, 8270 (2014).
- [23] K. Merkel, A. Kocot, J. K. Vij, P. J. Stevenson, A. Panov, and D. Rodriguez, Anomalous temperature dependence of layer spacing of de Vries liquid crystals: Compensation model, *Appl. Phys. Lett.* **108**, 243301 (2016).
- [24] N. Yadav, V. P. Panov, V. Swaminathan, S. P. Sreenilayam, J. K. Vij, T. S. Perova, R. Dhar, A. Panov, D. Rodriguez-Lojo, and P. J. Stevenson, Chiral smectic-A and smectic-C phases with de Vries characteristics, *Phys. Rev. E* **95**, 062704 (2017).
- [25] J. C. Roberts, N. Kapernaum, Q. Song, D. Nonnenmacher, K. Ayub, F. Giesselmann, and R. P. Lemieux, Design of liquid crystals with "de Vries-like" properties: Frustration between SmA- and SmC-promoting elements, *J. Am. Chem. Soc.* **132**, 364 (2010).
- [26] J. A. McCubbin, X. Tong, Y. Zhao, V. Snieckus, and R. P. Lemieux, Directed metalation-cross coupling route to ferroelectric liquid crystals with a chiral fluorenol core: The effect of intermolecular hydrogen bonding on polar order, *Chem. Mater.* **17**, 2574 (2005).
- [27] J. W. Goodby, E. Chin, J. M. Geary, J. S. Patel, and P. L. Finn, The ferroelectric liquid-crystalline properties of some chiral alkyl 4-n-alkanoyloxybiphenyl-4'-carboxylates, *J. Chem. Soc., Faraday Trans. 1: Phys. Chem. Condens. Phases* **83**, 3429 (1987).
- [28] Q. Song, D. Nonnenmacher, F. Giesselmann, and R. P. Lemieux, Tuning 'de Vries-like' properties in siloxane- and carbosilane-terminated smectic liquid crystals, *J. Mater. Chem. C* **1**, 343 (2013).
- [29] G. Galli, M. Reihmann, A. Crudeli, E. Chiellini, Y. P. Panarin, J. K. Vij, C. Blanc, V. Lorman, and N. Olsson, Design of siloxane liquid crystals forming a de Vries SmA* phase, *Mol. Cryst. Liq. Cryst.* **439**, 2111 (2005).
- [30] N. Hayashi, A. Kocot, M. J. Linehan, A. Fukuda, J. K. Vij, G. Heppke, J. Naciri, S. Kawada, and S. Kondoh, Experimental demonstration, using polarized Raman and infrared spectroscopy, that both conventional and de Vries smectic-A phases may exist in smectic liquid crystals with a first-order A-C* transition, *Phys. Rev. E* **74**, 051706 (2006).
- [31] A. A. Sigarev, J. K. Vij, Y. P. Panarin, P. Rudquist, S. T. Lagerwall, and G. Heppke, Molecular arrangement in a chiral smectic liquid crystal cell studied by polarized infrared spectroscopy, *Liq. Cryst.* **30**, 149 (2003).
- [32] R. Korlacki, A. Fukuda, J. K. Vij, A. Kocot, V. Görtz, M. Hird, and J. W. Goodby, Self-assembly of biaxial ordering and molecular tilt angle of chiral smectic liquid crystals in homeotropically aligned cells investigated using infrared spectroscopy, *Phys. Rev. E* **72**, 041704 (2005).
- [33] I. Chirtoc, M. Chirtoc, C. Glorieux, and J. Thoen, Determination of the order parameter and its critical exponent for nCB ($n = 5-8$) liquid crystals from refractive index data, *Liq. Cryst.* **31**, 229 (2004).
- [34] B. K. P. Scaife and J. K. Vij, Propagation of an electromagnetic wave in an absorbing anisotropic medium and infrared transmission spectroscopy of liquid crystals, *J. Chem. Phys.* **122**, 174901 (2005).
- [35] K. Merkel, A. Kocot, J. K. Vij, G. H. Mehl, and T. Meyer, The orientational order parameters of a dendritic liquid crystal organo-siloxane tetrapode oligomer, determined using polarized infrared spectroscopy, *J. Chem. Phys.* **121**, 5012 (2004); O. E. Kalinovskaya, Y. P. Panarin, and J. K. Vij, FTIR study of a chiral tilted SmA liquid crystalline phase, *Europhys. Lett.* **57**, 184 (2002).
- [36] M. S. Spector, P. A. Heiney, J. Naciri, B. T. Weslowski, D. B. Holt, and R. Shashidhar, Electroclinic liquid crystals with large induced tilt angle and small layer contraction, *Phys. Rev. E* **61**, 1579 (2000).
- [37] J. V. Selinger, P. J. Collings, and R. Shashidhar, Field-dependent tilt and birefringence of electroclinic liquid crystals: Theory and experiment, *Phys. Rev. E* **64**, 061705 (2001).
- [38] S. Inui, N. Iimura, T. Suzuki, H. Iwane, K. Miyachi, Y. Takanishi, and A. Fukuda, Thresholdless antiferroelectricity in liquid crystals and its application to displays, *J. Mater. Chem.* **6**, 671 (1996).
- [39] N. A. Clark, T. Bellini, R. F. Shao, D. Coleman, S. Bardon, D. R. Link, J. E. MacLennan, X. H. Chen, M. D. Wand, D. M. Walba, P. Rudquist, and S. T. Lagerwall, Electro-optic characteristics

- of de Vries tilted smectic liquid crystals: Analog behavior in the smectic A^* and smectic C^* phases, *Appl. Phys. Lett.* **80**, 4097 (2002).
- [40] Y. Q. Shen, L. X. Wang, R. F. Shao, T. Gong, C. H. Zhu, H. Yang, J. E. MacLennan, D. M. Walba, and N. A. Clark, Generalized Langevin-Debye model of the field dependence of tilt, birefringence, and polarization current near the de Vries smectic- A^* to smectic- C^* liquid crystal phase transition, *Phys. Rev. E* **88**, 062504 (2013).
- [41] V. Swaminathan, V. P. Panov, Y. P. Panarin, S. P. Sreenilayam, J. K. Vij, A. Panov, D. Rodriguez-Lojo, P. J. Stevenson, and E. Gorecka, The effect of chiral doping in achiral smectic liquid crystals on the de Vries characteristics: Smectic layer thickness, electro-optics and birefringence, *Liq. Cryst.* **45**, 513 (2018).
- [42] V. Swaminathan, V. P. Panov, A. Panov, D. Rodriguez-Lojo, P. J. Stevenson, E. Gorecka, and J. K. Vij, Design and electro-optic investigations of de Vries smectics for exhibiting broad temperature ranges of SmA^* and SmC^* phases and fast electro-optic switching (unpublished).
- [43] S. T. Lagerwall, P. Rudquist, and F. Giesselmann, The orientational order in so-called de Vries materials, *Mol. Cryst. Liq. Cryst.* **510**, 148 (2009).
- [44] D. M. Agra-Kooijman, H. Yoon, S. Dey, and S. Kumar, Origin of weak layer contraction in de Vries smectic liquid crystals, *Phys. Rev. E* **89**, 032506 (2014).
- [45] K. Saunders, D. Hernandez, S. Pearson, and J. Toner, Disordering to Order: de Vries Behavior from a Landau Theory for Smectic Phases, *Phys. Rev. Lett.* **98**, 197801 (2007).
- [46] A. Kocot, R. Wrzalik, J. K. Vij, and R. Zentel, Pyroelectric and electro-optical effects in the SmC^* phase of a polysiloxane liquid crystal, *J. Appl. Phys.* **75**, 728 (1994).